Edc3p and a glutamine/asparagine-rich domain of Lsm4p function in processing body assembly in *Saccharomyces cerevisiae*

Carolyn J. Decker, Daniela Teixeira, and Roy Parker

Department of Molecular and Cellular Biology and Howard Hughes Medical Institute, University of Arizona, Tucson, AZ 85721

Processing bodies (P-bodies) are cytoplasmic RNA granules that contain translationally repressed messenger ribonucleoproteins (mRNPs) and messenger RNA (mRNA) decay factors. The physical interactions that form the individual mRNPs within P-bodies and how those mRNPs assemble into larger P-bodies are unresolved. We identify direct protein interactions that could contribute to the formation of an mRNP complex that consists of core P-body components. Additionally, we demonstrate that the formation of P-bodies that are visible by light microscopy occurs either through Edc3p, which acts as a scaffold and cross-bridging protein, or via the "prionlike" domain in Lsm4p. Analysis of cells defective in P-body formation indicates that the concentration of translationally repressed mRNPs and decay factors into microscopically visible P-bodies is not necessary for basal control of translation repression and mRNA decay. These results suggest a stepwise model for P-body assembly with the initial formation of a core mRNA–protein complex that then aggregates through multiple specific mechanisms.

Introduction

An important aspect of the control of eukaryotic gene expression is the regulation of the mRNA translation and degradation, which are often intertwined. The control of translation and mRNA degradation can involve conserved cytoplasmic RNA granules, which are defined as microscopically visible granules containing mRNA and proteins (Anderson and Kedersha, 2006). One class of cytoplasmic RNA granule is termed a processing body (P-body). P-bodies are dynamic aggregates of untranslating mRNA in conjunction with translation repressors and mRNA degradation components (Eulalio et al., 2007a; Parker and Sheth, 2007). P-bodies and the mRNPs assembled within them are of interest because they have been implicated in translation repression (Holmes et al., 2004; Coller and Parker, 2005), normal mRNA decay (Sheth and Parker, 2003; Cougot et al., 2004), nonsense-mediated decay (Unterholzner and Izaurralde, 2004; Sheth and Parker, 2006), microRNA (miRNA)-mediated repression (Liu et al., 2005; Pillai et al., 2005), and mRNA storage (Brengues et al., 2005; Bhattacharyya et al., 2006). In addition, P-bodies are related to cytoplasmic RNA granules containing translationally repressed mRNPs found in germ cells and neurons (Barbee et al., 2006; Seydoux and Braun, 2006).

The mechanisms by which P-bodies form are largely unknown. For example, the specific protein–protein and protein–RNA interactions that mediate the formation of an mRNP that is capable of being incorporated into a P-body are unclear. Similarly, the interactions that mediate the aggregation of mRNPs together into microscopically visible structures are unknown. An important issue is to understand how P-bodies assemble and what the consequences of different scales of assembly are to the translation and degradation of mRNA.

P-bodies in yeast through mammals contain a conserved core of proteins (Anderson and Kedersha, 2006; Eulalio et al., 2007a; Parker and Sheth, 2007). Some of these core proteins are involved in mRNA degradation, including the decapping enzyme Dcp1p/Dcp2p, the exonuclease Xrn1p, the Ccr4p–Pop2–Notp deadenylase complex, and the decapping activators Dhh1p, Pat1p, Lsm1-7p, and Edc3p. Some of these proteins, like Dhh1p and Pat1p, have also been implicated in translation repression (Holmes et al., 2004; Coller and Parker, 2005). Metazoan P-bodies contain additional components, including proteins involved in miRNA-mediated repression such as argonaute, GW182, and Mov10 (Anderson and Kedersha, 2006; Eulalio et al., 2007a; Parker and Sheth, 2007).

Correspondence to R. Parker: rrparker@u.arizona.edu

D. Teixeira's present address is Instituto de Ciencias Biomedica Abel Salazar, Universidade do Porto, Porto 4099-003, Portugal.

Abbreviations used in this paper: miRNA, microRNA; P-body, processing body; Q/N, glutamine/asparagine; SC, synthetic medium; YP, yeast extract/peptone medium.

The online version of this article contains supplemental material.

© The Rockefeller University Press $30.00
The Journal of Cell Biology, Vol. 179, No. 3, November 5, 2007 437–449
http://www.jcb.org/cgi/doi/10.1083/jcb.200704147

Several proteins have been implicated in P-body assembly. For example, in mammalian cells, P-bodies are greatly reduced by knockdown of GW182, RCK/p54, RAP55, Lsm4, Lsm1, Hedls/Ge-1, 4E-T, or miRNA biogenesis in general (Andrei et al., 2005; Ferraiuolo et al., 2005; Jakymiw et al., 2005; Chu and Rana, 2006; Pauley et al., 2006). However, because translation and P-body formation compete with each other, the lack of a specific protein can affect P-body formation by either reducing the pool of nontranslating mRNA or decreasing the aggregation of nontranslating mRNPs into P-bodies. Strikingly, P-bodies are restored when translation initiation is inhibited by arsenite in mammalian cells depleted of Lsm4 (Kedersha et al., 2005). This observation argues that Lsm4, and possibly some of the other mammalian factors as well, is not required for P-body assembly per se, but instead contributes to P-body formation by increasing the pool of translationally repressed mRNA. Thus, to understand how P-bodies form, it is important to distinguish whether a component functions in translation repression or in the actual aggregation of mRNPs with each other.

Genetic analyses of P-body assembly in yeast revealed that certain components are dependent on one another for their association with P-bodies and suggested that P-body formation was redundant, with partial roles being played by Dcp2p and Pat1p (Teixeira and Parker, 2007). However, the role of the P-body component Edc3p was not investigated. By analyzing the role of Edc3p in P-body assembly, we identified direct physical interactions between components of yeast P-bodies that, in combination with previous observations, lead to a model for the core mRNP structure within P-bodies. We also demonstrated that these core mRNPs, or small mRNP complexes, can be aggregated into microscopically visible P-bodies either through Edc3p acting as a scaffold protein and interacting with itself to interconnect mRNPs or by an aggregation mechanism dependent on the glutamine/asparagine (Q/N)-rich prionlike domain in Lsm4p. These results suggest a stepwise model for P-body assembly with the initial formation of a core mRNA–protein complex that then aggregates through multiple specific mechanisms.

Results

Edc3p functions in P-body formation

To test the role of Edc3p in P-body assembly, we examined the ability of *edc3Δ* strains to form P-bodies. In *edc3Δ* strains, Dcp1pGFP and Dcp2pGFP were no longer seen in the small P-bodies normally observed in mid-log cultures in wild-type strains (Fig. 1 A, left). Moreover, during glucose deprivation, where P-bodies are large (Teixeira et al., 2005), we observed that *edc3Δ* strains showed a strong reduction in the accumulation of multiple proteins into microscopically visible P-bodies (Fig. 1 A, left), although some P-bodies could still form (see the following paragraph). The *edc3Δ* strain also showed reduced P-body assembly in response to osmotic stress and in the stationary phase (not depicted). It should be noted that we were unable to determine if P-bodies too small to be detected in the light microscope were forming (see Discussion). Nevertheless, the strong reduction of P-bodies, as judged by six different proteins and under different growth conditions, indicates that Edc3p affects the formation of P-bodies.

We observed that the magnitude of the reduction of P-bodies in the *edc3Δ* strain was dependent on the experimental conditions used. Most strikingly, if aeration was limited during glucose deprivation, Edc3p was required for P-body accumulation (Fig. 2 A). In contrast, if cells were deprived of glucose while being strongly aerated, *edc3Δ* strains still formed P-bodies, although at reduced levels compared with wild-type cells (Fig. 2 A). These results suggested that there is also an Edc3-independent mode for forming P-bodies that is dependent on mitochondrial respiration. To test this possibility, we isolated and examined petite versions of wild-type and *edc3Δ* strains that are respiratory deficient (Fox et al., 1991). P-bodies increased in response to glucose deprivation in respiratory-deficient, but otherwise wild-type, cells, as judged by the increase in Dcp2GFP and Dhh1GFP foci (Fig. 2 A). In contrast, no Dcp2GFP or Dhh1GFP foci were observed after glucose removal in the *edc3Δ* strain that was respiratory deficient (Fig. 2 A). These results indicate that Edc3p plays a role in P-body assembly, although there is a second respiration-dependent mechanism during glucose deprivation that can contribute to P-body assembly.

Additional evidence that Edc3p affects, but is not required for, P-body assembly is that the large P-bodies that form in *dcp1Δ* or *xrn1Δ* strains because of the resulting defects in decapping and 5′-to-3′ degradation (Sheth and Parker, 2003; Teixeira and Parker, 2007) are reduced but not eliminated in *dcp1Δ edc3Δ* and *xrn1Δ edc3Δ* strains (Fig. 1 B).

Edc3p is required for P-body assembly but not for translation repression

The strong reduction of P-bodies in the respiratory-deficient *edc3Δ* strain during glucose deprivation suggests that Edc3p could either be required for the aggregation of mRNPs into P-bodies or for translational repression during glucose deprivation. To distinguish these two possibilities, we examined whether the respiratory-deficient *edc3Δ* strain could repress translation during glucose deprivation, as judged by polysome analysis.

We observed that both respiratory-deficient wild-type or *edc3Δ* cells showed a similar reduction in polysomes during glucose deprivation (Fig. 2 B). Because Edc3p is required for P-body formation under these conditions, this observation indicates that Edc3p primarily functions in the aggregation of nontranslating mRNPs into P-bodies. This result also implies that aggregation of mRNPs into microscopically visible P-bodies is not required for translation repression, at least in response to glucose deprivation.

Different domains of Edc3p interact with Edc3p, Dcp2p, and Dhh1p

These results identify Edc3p as a factor that contributes to the assembly of microscopically visible P-bodies. Edc3p is a member of the Lsm16 family of proteins and contains at its N terminus a divergent Lsm, or like-Sm, domain, a central FDF domain of unknown function containing the amino acid motif FDF, and a C-terminal YjeF-N domain that resembles the N-terminal domain of the *Escherichia coli* Yjef protein (Albrecht and Lengauer, 2004;

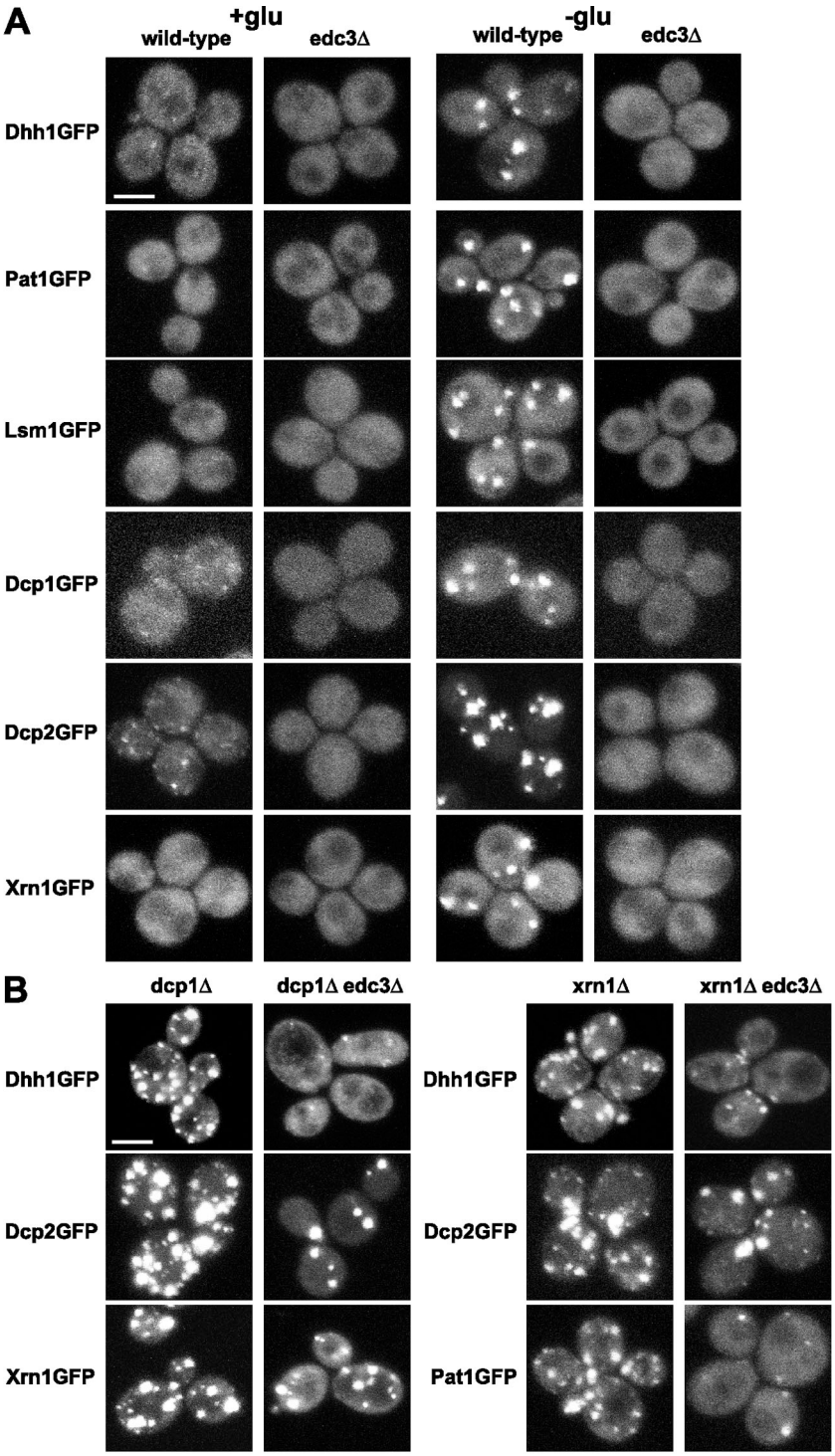

Figure 1. **Edc3p is important for P-body assembly.** (A) Localization of Dhh1GFP, Pat1GFP, Lsm1GFP, Dcp-1GFP, Dcp2GFP, and Xrn1GFP in wild-type and *edc3Δ* strains during exponential growth in YP with (+glu) or without (−glu) glucose for 10 min. (B) Localization of Dhh1GFP, Dcp2GFP, and Xrn1GFP in *dcp1Δ* or *dcp1Δ edc3Δ* strains or Dhh1GFP, Dcp2GFP, and Pat-1GFP in *xrn1Δ* or *xrn1Δ edc3Δ* strains during exponential growth in YP containing glucose. Bars, 3 μm.

Anantharaman and Aravind, 2004). To determine how these different Edc3 domains contribute to P-body assembly, we examined the interactions of each of these domains in two-hybrid tests with other P-body components and verified interactions by direct binding experiments with recombinant proteins.

In two-hybrid assays (Fig. 3 A), full-length Edc3p interacted with Edc3p, Dcp1p, the C-terminal structural domain of Dhh1p (Cheng et al., 2005), and the conserved region of Dcp2p (amino acids 1–300). The conserved region of Dcp2p is composed of two distinct structural domains: an N-terminal domain that interacts with Dcp1p and a C-terminal domain that contains the catalytic site (She et al., 2006). The C-terminal catalytic domain of Dcp2p encompassing amino acids 102–300 was sufficient to interact with full-length Edc3p. Subsequent experiments revealed that each of these interactions involved a specific domain of Edc3p.

Two observations indicate that the catalytic domain of Dcp2p (residues 102–300) primarily interacts with the Lsm

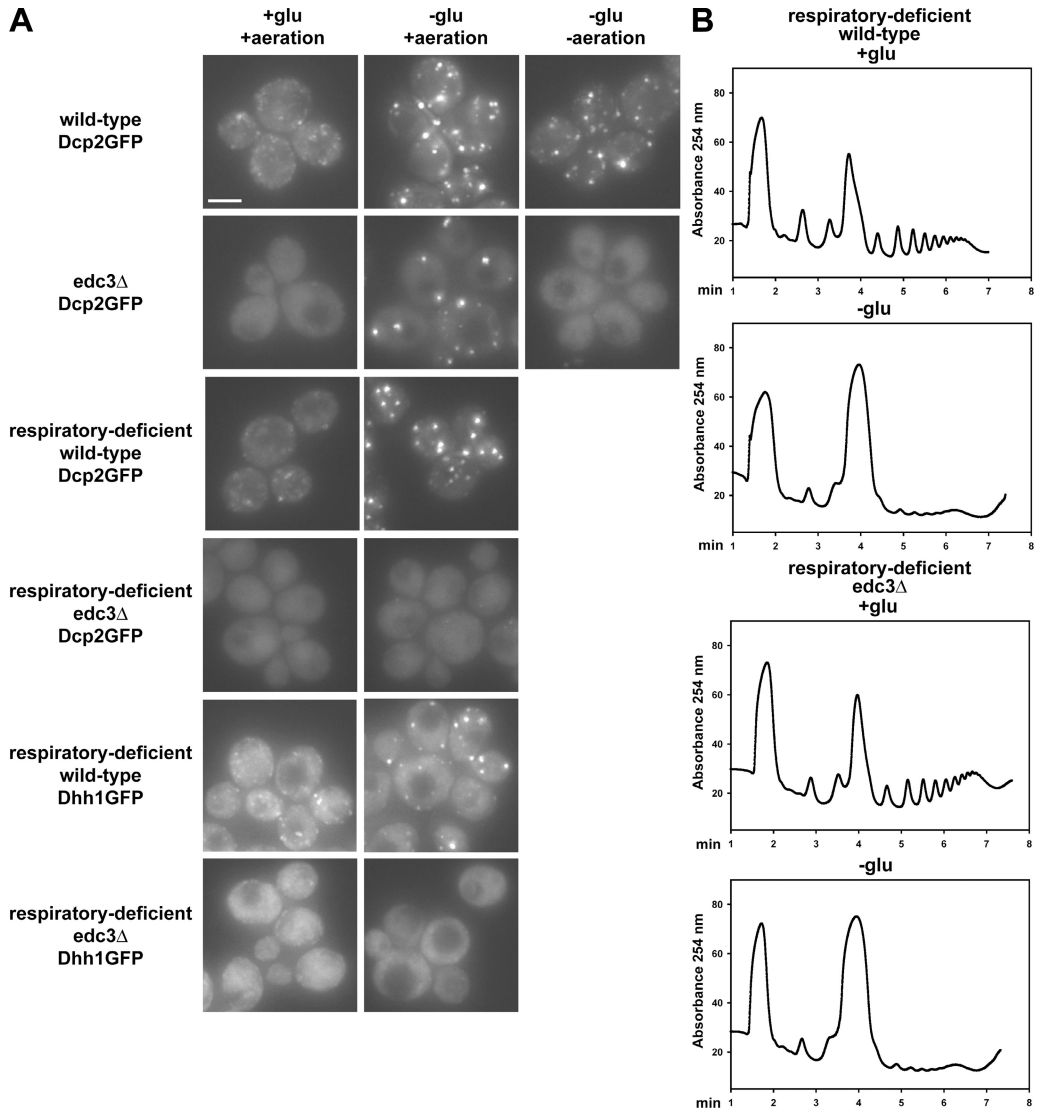

Figure 2. **When cells are unable to respire, Edc3p is required for P-body assembly, but not for translation repression, in response to glucose deprivation.** (A) Localization of Dcp2GFP or Dhh1GFP in respiratory-competent or -deficient wild-type or *edc3Δ* strains during exponential growth in YP containing glucose (+glu, +aeration), deprived of glucose for 10 min while being aerated (−glu, +aeration), or deprived of glucose for 10 min while concentrated in a microcentrifuge tube (−glu, −aeration). Bar, 3 μm. (B) Polysome profiles, A254 traces of sucrose density gradients, were obtained from respiratory-deficient wild-type or *edc3Δ* strains grown under standard growth conditions (+glu) or deprived of glucose for 10 min while being aerated (−glu).

domain of Edc3p. First, the Lsm domain is sufficient in the two-hybrid assay to interact with residues 102–300 of Dcp2p (Fig. 3 A). Second, a His-tagged Lsm domain binds to recombinant Flag-tagged Dcp2p (either 1–300 or 102–300) in an in vitro pull-down assay from bacterial lysates (Fig. 3 B). Lysates were used because the Lsm domain became insoluble when concentrated during purification. The Lsm domain was not pelleted by the anti-Flag resin alone (Fig. 3 B) or by GST-tagged Dhh1p (Fig. 3 D), indicating that the Lsm domain–Dcp2p interaction is specific. These results identify the Lsm domain as a region of Edc3p that directly binds the catalytic domain of Dcp2p.

Two observations indicate that Dcp2p also interacts with the FDF domain of Edc3p. First, although the FDF domain is not sufficient for a two-hybrid interaction with Dcp2p, a combined Lsm–FDF construct shows a stronger interaction with the catalytic domain of Dcp2p than just the Lsm domain (Fig. 3 A). Second, the purified FDF domain could be affinity purified with both the Flag-tagged 1–300–amino acid fragment and the 102–300–amino acid fragment of Dcp2p, although this interaction is sensitive to moderate salt (Fig. 3 C). These results identify the FDF domain as a region that can directly bind Dcp2p, albeit weakly.

Two observations indicate that the FDF domain can directly interact with the C-terminal domain of Dhh1p as well. First, the FDF domain was sufficient in two-hybrid experiments to interact with this portion of Dhh1p (Fig. 3 A). Second, recombinant Dhh1p interacted with recombinant FDF domain in an in vitro pull-down assay (Fig. 3 E). Moreover, the in vitro interaction between the FDF domain and Dhh1p only required the C-terminal domain of Dhh1p (Fig. 3 E). In contrast, purified Dhh1p failed to interact with the Lsm domain of Edc3p in pull-down experiments (Fig. 3 D). These results identify the FDF domain as a site that directly binds Dhh1p.

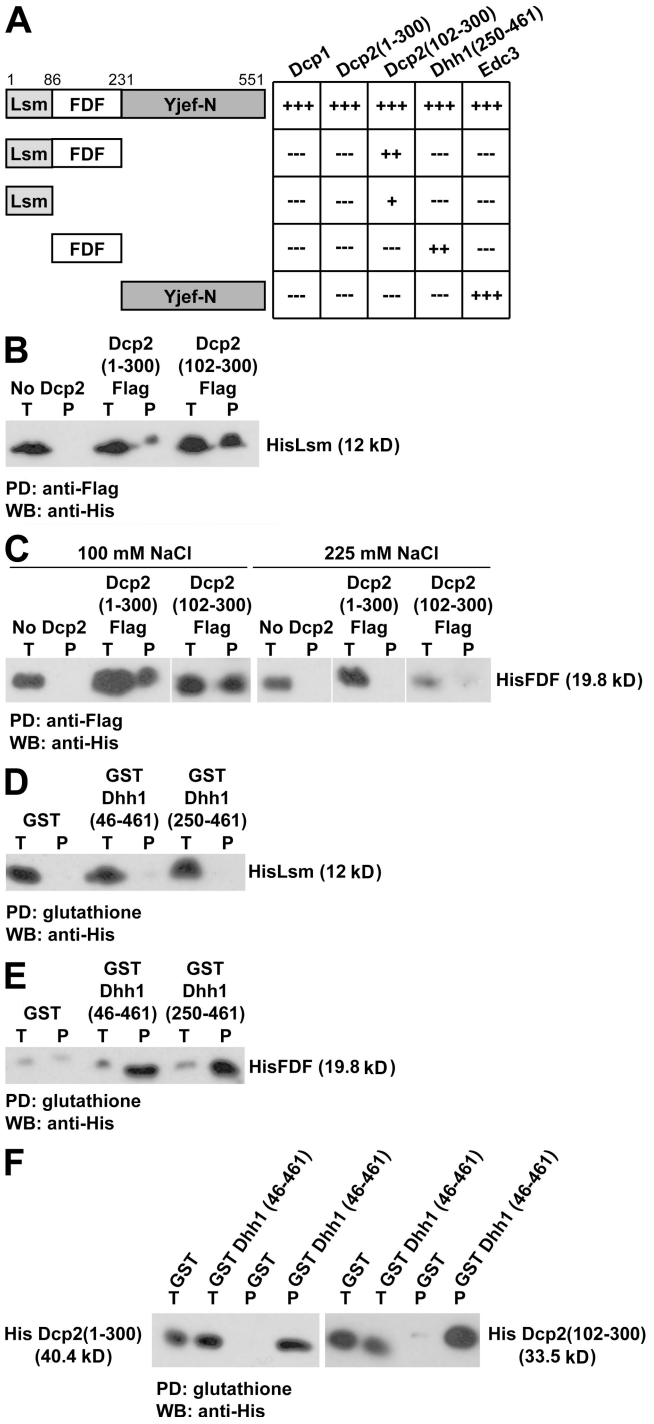

Figure 3. **Edc3p interacts with itself, Dcp2p, and Dhh1p through distinct domains.** (A) Summary of two-hybrid protein interaction assays between full-length or the indicated deleted versions of Edc3p and full-length Dcp1p or Edc3p, the conserved region of Dcp2p (amino acids 1–300), the catalytic domain of Dcp2p (amino acids 102–300), or a C-terminal fragment of Dhh1p (amino acids 250–461). +++, ++, and + indicate relative positive interaction based on β-galactosidase assays. — indicates no detectable interaction. (B) An in vitro binding assay between purified His-Dcp2(1–300)-Flag or His-Dcp2(102–300)-Flag and *E. coli* lysate containing the His-tagged Lsm domain of Edc3p in the presence of 225 mM NaCl. Anti-Flag affinity resin was used to pull down (PD) the Flag-tagged Dcp2 proteins and anti-His antibody used in Western blots (WB) to detect the His-tagged Lsm domain. Total (T) lanes represent 1/8 of the material loaded in the pellet (P) lanes. (C) An in vitro binding assay between purified His-Dcp2(1–300)-Flag or His-Dcp2(102–300)-Flag and a purified His-tagged FDF domain of Edc3p in the presence of 100 or 225 mM NaCl. Total lanes represent 1/8 of the material loaded in the pellet lanes. (D) An in vitro binding assay between purified GST, GST-tagged Dhh1(46–461) or Dhh1(250–461), and an *E. coli* lysate containing a His-tagged Lsm domain of Edc3p. Glutathione-Sepharose was used to pull down the GST-tagged Dhh1 proteins and anti-His antibody was used in Western blots to detect the His-tagged Lsm domain. Total lanes represent 1/8 of the material loaded in the pellet lanes. (E) An in vitro binding assay between purified GST, GST-tagged Dhh1(46–461) or Dhh1(250–461), and a purified His-tagged FDF domain of Edc3p. Total lanes represent 1/8 of the material loaded in the pellet lanes. (F) An in vitro binding assay between purified GST or GST-tagged Dhh1(46–461) and His-Dcp2(1–300)-Flag or His-Dcp2(102–300)-Flag. Glutathione-Sepharose was used to pull down the GST-tagged Dhh1 protein and anti-His antibody used in Western blots to detect the His-tagged Dcp2 proteins. Total lanes represent 1/8 of the material loaded in the pellet lanes.

The YjeF-N domain of Edc3p can interact with itself and was sufficient to interact with Edc3p (Fig. 3 A). This is consistent with genome-wide analyses that have identified the C terminus of Edc3p as being sufficient to interact with itself by two-hybrid or phage display experiments (Fromont-Racine et al., 2000; Marino-Ramirez and Hu, 2002).

We also obtained evidence that the C-terminal domain of Dhh1p binds directly to the catalytic domain of Dcp2p. Specifically, we observed a two-hybrid interaction between these domains of Dhh1p and Dcp2p (unpublished data). In addition, in binding experiments with purified recombinant proteins, GST-tagged Dhh1p pulled down Dcp2p (Fig. 3 F), and reciprocally GST-tagged Dhh1p was pulled down by Flag-tagged Dcp2p (not depicted). In these experiments, the catalytic domain of Dcp2p (residues 102–300) was sufficient to bind to Dhh1p (Fig. 3 F). In addition, the C-terminal domain, but not the N-terminal domain, of Dhh1p was sufficient to bind to Dcp2p (unpublished data). These data indicate that the C-terminal domain of Dhh1p directly interacts with the catalytic domain of Dcp2p.

The Lsm and Yjef-N domains of Edc3p are required for its function in the formation of microscopically visible P-bodies

These results identify three different domains of Edc3p that interact with specific P-body components. To determine how these domains contribute to P-body formation, we deleted each domain of Edc3p and asked if the mutant protein could rescue the P-body aggregation defect of the respiratory-deficient *edc3Δ* strain, where P-body formation is strongly dependent on Edc3p. We examined the formation of Dcp2GFP foci in both exponentially growing cells and during glucose deprivation. As expected, expression of full-length Edc3p complemented the P-body aggregation defect of the *edc3Δ* strain under both conditions (Fig. 4). Edc3p lacking the FDF domain functioned in P-body assembly (Fig. 4). In contrast, deletion of either the Lsm or Yjef-N domains caused defects in the formation of Dcp2GFP (Fig. 4) and Dhh1GFP foci (Fig. S1, available at http://www.jcb.org/cgi/content/full/jcb.200704147/DC1) both in exponentially growing cells and under glucose deprivation. The defect in P-body aggregation in cells expressing the ΔLsm and ΔYjef-N proteins was not simply caused by decreased expression because the amount of these mutant proteins was not substantially decreased relative to full-length Edc3p (Fig. S2, A and B).

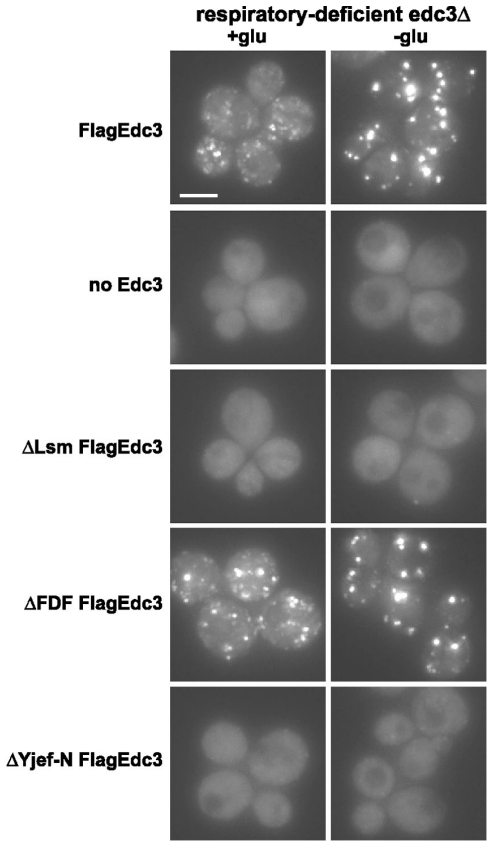

Figure 4. **The Lsm and Yjef-N domains are required for Edc3p to function in P-body assembly.** Localization of Dcp2GFP in a respiratory-deficient *edc3Δ* strain expressing from a plasmid Flag-tagged full-length Edc3p, no Edc3p, or versions of Flag-tagged Edc3p in which the Lsm, FDF, or Yjef-N domains were deleted during exponential growth in SC containing glucose (+glu) or after being deprived of glucose for 10 min under aeration (−glu). Bar, 3 μm.

Moreover, the decrease in Dcp2GFP foci was not caused by the deletion of the Lsm or Yjef-N domains of Edc3p reducing the levels of Dcp2 protein (Fig. S2 C). These results identify the Lsm and Yjef-N domains of Edc3p as being required for P-body aggregation and suggest that Edc3p acts as a scaffold protein that links multiple mRNPs together.

The Q/N-rich prionlike domain of Lsm4p is required for P-body assembly in the absence of Edc3p

As described earlier, our analysis indicated that there is also an Edc3-independent mechanism by which microscopically visible P-bodies can form. Interestingly, a component of the Lsm1-7p complex, Lsm4p, has a C-terminal Q/N-rich domain, which has been categorized as a prionlike domain (Michelitsch and Weissman, 2000). Moreover, Lsm4p can function in a similar manner to known yeast prion proteins in that it can induce the [PSI+] prion when overexpressed (Derkatch et al., 2001). Thus, we hypothesized that the Edc3p-independent mode of P-body aggregation might involve the Lsm4p Q/N-rich domain. To test this model, we deleted the C-terminal 97 amino acids encompassing the Q/N-rich sequence within Lsm4p and assayed the effect of this deletion on P-body formation in the absence of Edc3p. The *lsm4ΔC* and *lsm4ΔC edc3Δ* strains were viable, indicating that the truncated protein is being expressed because Lsm4p is essential.

An important result was that the *lsm4ΔC edc3Δ* strain was defective in P-body formation during glucose deprivation (Fig. 5 A, right). In contrast, deletion of the C terminus of Lsm4 protein by itself did not reduce P-bodies during mid-log growth or have a strong effect on P-body formation in response to glucose deprivation (Fig. 5 A). This result indicates that either Edc3p or the prionlike domain of Lsm4p is sufficient for P-body aggregation during glucose deprivation. It should be noted that small Dcp2GFP foci were occasionally observed in the *lsm4ΔC edc3Δ* strain, indicating that microscopically visible P-bodies can assemble, though inefficiently, in the absence of both Edc3p and the C terminus of Lsm4p. Nevertheless, the severe defect in P-body formation in the *lsm4ΔC edc3Δ* mutant identifies the Q/N-rich domain of Lsm4p as a second protein domain that can affect the formation of microscopically visible P-bodies.

Because Dcp2GFP was used as a marker for P-bodies, it was formally possible that the Q/N-rich domain of Lsm4p was solely required for the localization of Dcp2p to P-bodies in the absence of Edc3p. To verify that the *lsm4ΔC edc3Δ* deletion mutant was defective for P-body formation, we examined the localization of the reporter mRNA MFA2P-U1A, which contains binding sites for the U1A protein by coexpressing U1A protein fused to GFP. This reporter mRNA accumulates in P-bodies after glucose deprivation (Brengues et al., 2005). As shown in Fig. 5 B, the *lsm4ΔC edc3Δ* mutant has a severe defect in the accumulation of the MFA2P-U1A reporter mRNA in response to glucose deprivation. This observation supports the interpretation that both the Q/N-rich domains of Lsm4p and Edc3p contribute to P-body formation.

The Q/N domain of Lsm4p could affect P-body formation by being required for translation repression during glucose deprivation in the *edc3Δ* strain or the aggregation of translationally repressed mRNPs in the absence of Edc3p. To distinguish these two possibilities, we examined the extent of translation repression in the *lsm4ΔC edc3Δ* strain during glucose deprivation. We observed that deletion of the Lsm4 prionlike domain in combination with deletion of Edc3p did not interfere with translation repression under these conditions (Fig. 5 C). This indicates that the defect in P-body formation in the *lsm4ΔC edc3Δ* strain during glucose deprivation is not caused by a failure to repress translation. Thus, these results demonstrate that a second mechanism for P-body aggregation is based on the Lsm4 Q/N-rich domain.

The simplest model for how the Lsm4 Q/N-rich domain contributes to P-body formation is that it aggregates with itself, or other Q/N-rich domains, in a manner analogous to the assembly mechanism for Q/N-rich domains in known prions. However, given the dynamic and reversible nature of P-body assembly, such interactions mediated by the Lsm4 Q/N-rich domain would not be heritable like a classical prion. To test whether the Q/N-rich domain of Lsm4 functions analogously to a prion, we asked whether it could be substituted by the Q/N-rich prion domain of a known yeast prion protein, Rnq1p (Sondheimer and Lindquist, 2000). The C terminus of Lsm4p was replaced by the prion domain of Rnq1p, and the fusion protein

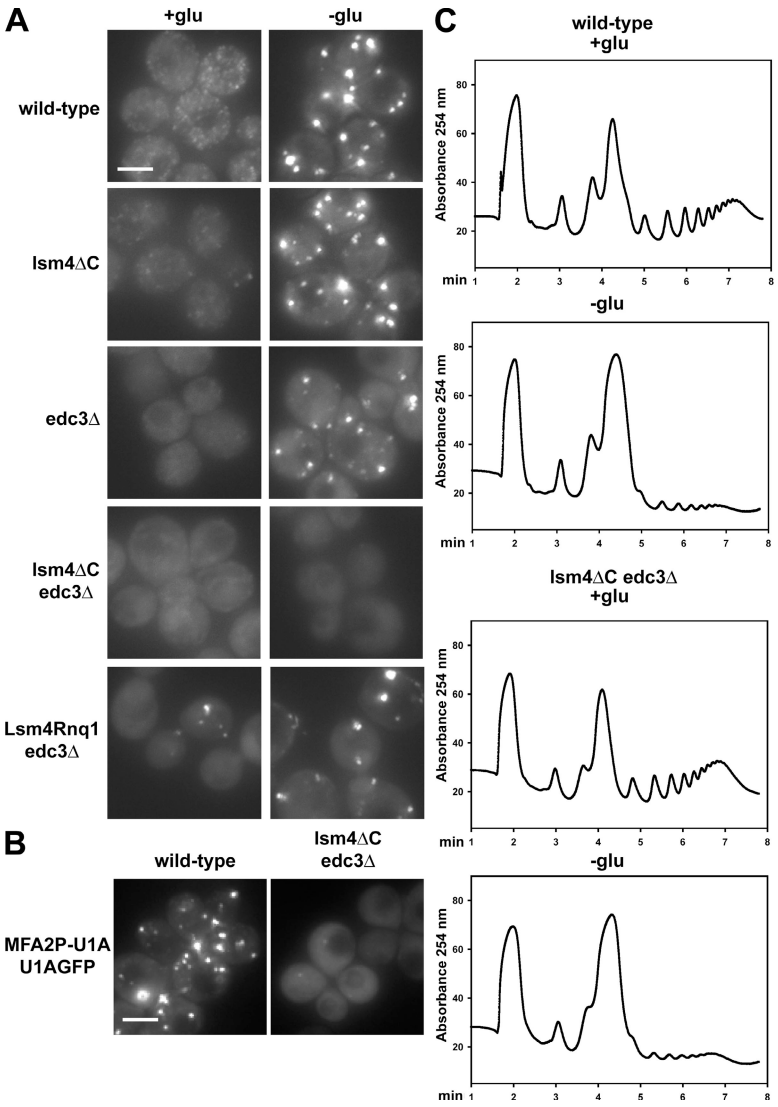

Figure 5. **In the absence of Edc3p, the prionlike domain of Lsm4p is required for P-body aggregation, but not for translation repression, in response to glucose deprivation.** (A) Localization of Dcp2GFP in wild-type, *edc3Δ*, *lsm4ΔC* (deletion of C terminus of Lsm4 including the Q/N-rich prionlike domain), or *lsm4ΔC edc3Δ* strains, or an *lsm4Δ edc3Δ* strain carrying a plasmid in which the C-terminal Q/N-rich domain of Lsm4p has been replaced with the prion domain of Rnq1p during exponential growth in YP containing glucose (+glu) or after being deprived of glucose for 10 min while being aerated (−glu). (B) Localization of MFA2P-U1A mRNA in wild-type or *lsm4ΔC edc3Δ* strains deprived of glucose for 10 min while being aerated. The MFA2P-U1A mRNA was detected by coexpressing U1A fused with GFP, which binds to the U1A binding sites within the 3′ UTR of the mRNA. Note that a different contrast range was used than the range in A because of the intense fluorescence signal of the RNA foci in the wild-type cells. Bars, 3 μm. (C) Polysome profiles, A254 traces of sucrose density gradients, obtained from wild-type or *lsm4ΔC edc3Δ* strains grown under standard growth conditions (+glu) or deprived of glucose for 10 min while being aerated (−glu).

was tested for its ability to form Dcp2GFP foci in cells lacking both Lsm4p and Edc3p. In the *lsm4Δ edc3Δ* strain expressing the Lsm4Rnq1 fusion protein, Dcp2GFP foci were observed in exponentially growing cells and were increased after glucose deprivation (Fig. 5 A, bottom). Thus, the prion domain of Rnq1p was able to functionally replace the Q/N-rich domain of Lsm4p for the assembly of P-bodies, which is consistent with Lsm4p promoting P-body assembly via a prionlike aggregation mechanism. Interestingly, the Dcp2GFP foci seen in exponentially growing cells expressing the Lsm4Rnq1 fusion protein were more intense than those seen in cells expressing wild-type Lsm4 protein. The ability of the Rnq1 Q/N-rich domain to enhance P-body formation during exponential growth argues that specific features of the Lsm4 Q/N-rich domain are required for the highly reversible nature of P-body formation.

Edc3p- and Lsm4p-driven aggregation does not substantially affect mRNA decay

Our results define two major mechanisms that allow the formation of microscopically visible P-bodies. This provides an opportunity to examine the functional significance of aggregation of mRNPs into larger P-body structures. Because the *lsm4ΔC edc3Δ* strain represses translation during glucose deprivation, but is severely defective in forming visible P-bodies, we conclude that the efficient assembly of large visible P-bodies is not required for translation repression during glucose deprivation. To examine how the formation of large P-bodies contributes to mRNA decapping, we examined the decay of two reporter mRNAs, MFA2pG and PGK1pG (Decker and Parker, 1993), in *edc3Δ*, *lsm4ΔC*, and *lsm4ΔC edc3Δ* strains as compared with the wild-type strain. Deletion of the Q/N-rich domain of Lsm4 protein and the Edc3 protein did not substantially alter the decay rate of the unstable MFA2pG mRNA (Fig. 6 A) or the stable PGK1pG mRNA (not depicted), indicating that mRNA turnover is not strongly affected in cells lacking both P-body aggregation mechanisms. This result indicates that the aggregation of mRNPs together into microscopically visible P-bodies is not necessary for the basal control of mRNA decay rates. This observation indicates that assembly of a transcript into an individual mRNP containing the mRNA decapping proteins or into small complexes not detected by light microscopy is sufficient for mRNA decapping under normal conditions (see Discussion).

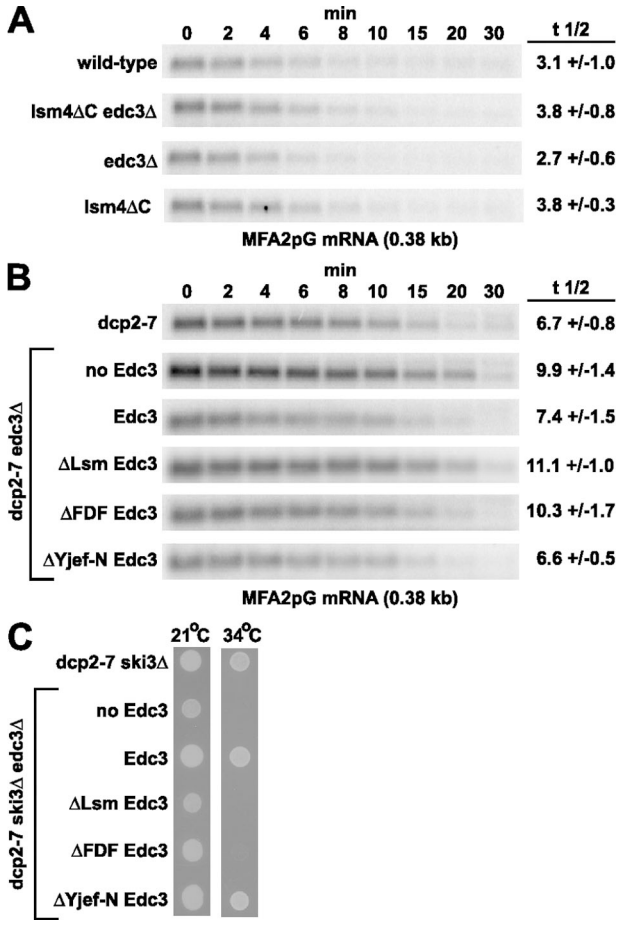

Figure 6. **P-body aggregation does not substantially affect mRNA decay.** (A) Decay analysis of MFA2pG mRNA in wild-type, *edc3Δ*, *lsm4ΔC*, or *lsm4ΔC edc3Δ* strains. Time points after transcriptional repression are indicated above each lane. The half-life values shown on the right are in minutes and represent the mean and SD based on three experiments. (B) Decay analysis of MFA2pG mRNA in *edc3Δ* or control strains carrying the temperature-sensitive allele dcp2-7 performed at 24°C, where dcp2-7 is partially active. The *dcp2-7 edc3Δ* strain contained plasmids expressing no Edc3p, Flag-tagged full-length Edc3p, or versions of Flag-tagged Edc3p in which the Lsm, FDF, or Yjef-N domains were deleted. The half-life values are in minutes and represent the mean and SD based on four experiments. (C) Growth of the *dcp2-7 ski3Δ* control strain or the *dcp2-7 ski3Δ edc3Δ* strain expressing no Edc3p, Flag-tagged full-length Edc3p, or versions of Flag-tagged Edc3p in which the Lsm, FDF, or Yjef-N domains were deleted on synthetic medium at 21 or 34°C.

The Edc3 protein is known to enhance decapping under conditions where decapping rates are compromised by the conditional allele of dcp2-7 (Kshirsagar and Parker, 2004). Given this, it was possible that the ability of Edc3p to enhance decapping by the dcp2-7 protein could result from its function in aggregating P-body components together, and thus concentrating decapping factors and substrate mRNA molecules together. Alternatively, because Dcp2p can interact directly with the Lsm and FDF domains of Edc3p, Edc3p might stimulate Dcp2p function by direct physical interactions.

To test whether P-body aggregation by Edc3p enhances decapping, we examined the ability of the different domain deletion mutants of Edc3p to complement the *edc3Δ* decapping defect seen in *dcp2-7* strains. As observed previously, *edc3Δ* exacerbates a partial defect in the decay of the MFA2pG mRNA at a low temperature caused by the temperature-sensitive allele dcp2-7 (Fig. 6 B). Deletion of *EDC3* also slows growth in *dcp2-7 ski3Δ* cells (Kshirsagar and Parker, 2004), in which 3′-to-5′ mRNA decay is inactive and decapping is partially defective because of the growth temperature (Fig. 6 C). An important result is that the Yjef-N deletion mutant complemented both the decay and growth defects caused by the absence of Edc3p (Fig. 6, B and C). Because the Yjef-N domain is necessary for P-body aggregation in exponentially growing cells, these results indicate that Edc3p's role in enhancing decay under these conditions is not dependent on its ability to form large P-body aggregates. In contrast, decay and growth were defective when either the ΔLsm or ΔFDF Edc3p variants were expressed (Fig. 6, B and C), which indicates that both the Lsm and FDF domains are necessary for Edc3p to enhance decapping. Because these are the domains that interact with Dcp2p and Dhh1p, this result suggests that Edc3p may enhance decapping by binding to and directly affecting the function of the decapping machinery.

Discussion

The formation of cytoplasmic P-bodies can be associated with translation repression and/or mRNA decapping and degradation. An unresolved issue is how P-bodies form and the functional significance of assembly into larger scale aggregates. In the simplest model, the formation of P-bodies can be considered to occur in at least two distinct steps: an initial step wherein an individual mRNA is associated with various proteins to form an mRNP capable of aggregation into a larger P-body, and a second step whereby individual mRNPs are then aggregated together to form P-bodies of sufficient size to be visible in the light microscope. However, it also remains possible that there are intermediate steps in the aggregation of mRNPs that can assemble collections of mRNPs too small to be seen in the light microscope. By examination of P-body formation in yeast, we were able to identify important interactions that promote P-body formation. These interactions suggest an initial model for P-body assembly involving interactions of subcomplexes of core P-body components with the mRNA and each other, followed by aggregation of individual mRNPs, or small complexes of mRNPs, into larger P-bodies by a self-interaction domain of Edc3p and the Q/N-rich C-terminal tail of Lsm4p.

Assembly of a core P-body mRNP

A first step in the formation of P-bodies is the assembly of individual mRNPs that contain P-body components. Our results, combined with previous observations described in this and the following paragraph, suggest a working model for the assembly of the core P-body components into a complex associated with mRNAs (Fig. 7). First, an initial step in P-body interaction could be the recruitment of the Dcp1, Dcp2, Edc3, and Dhh1 proteins to the mRNA, most likely as a protein complex. The existence of this complex is based on the direct protein interactions we observed between Dcp2p, Dhh1p, and Edc3p (Fig. 3). It should be noted that the interactions between Dcp2p, Dhh1p, and Edc3p may not occur simultaneously, given that they involve

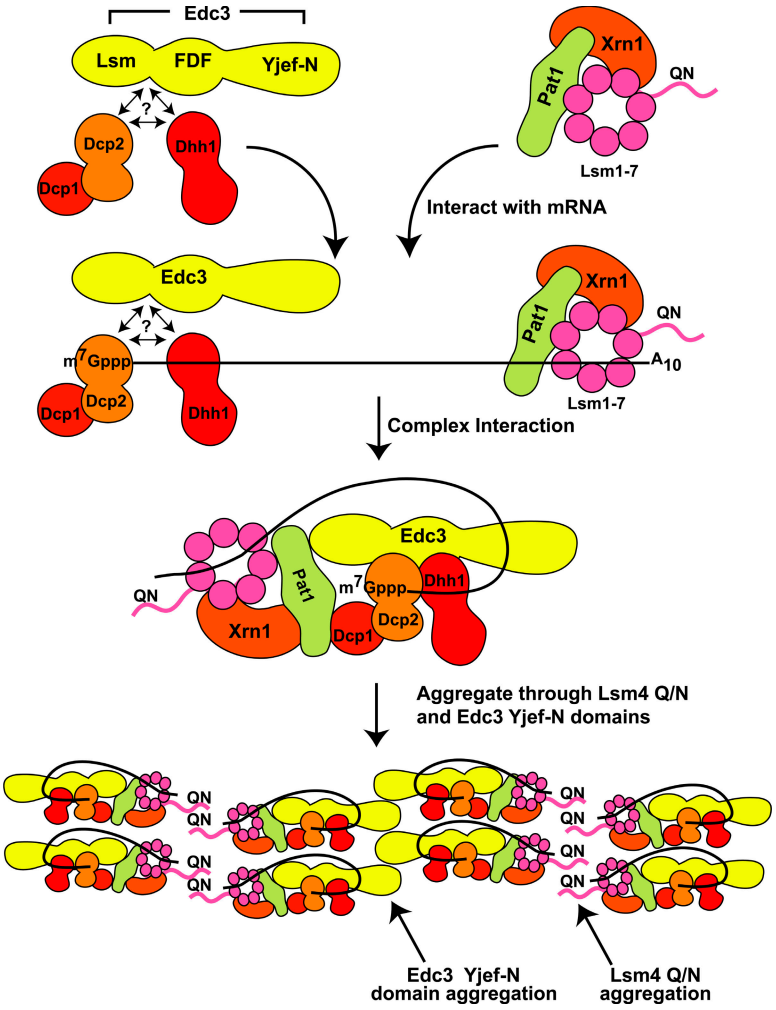

Figure 7. **Model for P-body assembly.** First, two subcomplexes of conserved "core" proteins assemble onto mRNA through a series of direct interactions between their components and with the mRNA. One of these subcomplexes is composed of Dcp1p, Dcp2p, Dhh1p, and Edc3p, although Dcp2, Dhh1p, and Edc3p may or may not bind simultaneously with each other. The other subcomplex consists of Pat1p, Lsm1-7p, and Xrn1p. Individual core P-body mRNPs could then potentially aggregate into larger assemblies through interactions dependent on the Edc3p YjeF-N domain and/or the Lsm4p Q/N-rich prionlike domain.

the same domains of Dcp2p and Dhh1p. Dcp1p is likely to be a component of this complex based on the direct physical interaction between yeast Dcp1p and Dcp2p (Steiger et al., 2003; She et al., 2006), which is required for Dcp1p to be recruited into P-bodies (Teixeira and Parker, 2007). Moreover, a complex of Dcp1p–Dcp2p–Edc3p purifies together from yeast (Gavin et al., 2006), and a similar complex copurifies from mammalian cells that includes the homologue of Dhh1p, Rck/p54, and an additional subunit, Ge-1 or Hedls (Fenger-Gron et al., 2005). Finally, Dcp1p, Dcp2p, Edc3p, and Dhh1p are recruited to P-bodies independently of other known P-body components (Teixeira and Parker, 2007). This suggests that one step in the formation of an mRNP that can accumulate in P-bodies is the recruitment of Dcp1p–Dcp2p–Edc3p–Dhh1p complexes to the mRNA.

Several observations suggest that a complex minimally consisting of Pat1p and the Lsm1-7p complex also associates with the mRNA during P-body assembly. First, Pat1p and the Lsm1-7p complex copurify from yeast (Bouveret et al., 2000; Tharun et al., 2000). Second, Pat1p is required for recruitment of the Lsm1-7p complex into P-bodies, and the deletion of Lsm1p affects the efficiency of Pat1p recruitment into P-bodies in part by shifting Pat1p into the nucleus (Teixeira and Parker, 2007). Xrn1p is also likely to be part of the Pat1p–Lsm1-7p complex because it can copurify with these proteins (Bouveret et al., 2000). Finally, the Pat1p–Lsm1-7p complex appears to function somewhat independently of the Dcp1p–Dcp2p–Edc3p–Dhh1p complex because Pat1p and Dhh1p can each independently target mRNAs to P-bodies when overexpressed (Coller and Parker, 2005).

We suggest that an individual P-body mRNP forms, at least in part, as a result of recruitment of the Dcp1p–Dcp2p–Edc3p–Dhh1p and Pat1p–Lsm1-7p–Xrn1p complexes to the mRNA, although their specific location on the mRNA remains to be determined. In addition, the two subcomplexes may directly interact with each other while bound to the mRNA based on the identification of interactions between Pat1p with Dcp1p and Edc3p (Pilkington, G., and R. Parker, personal communication). An unresolved issue is whether there are other RNA binding proteins bound to the mRNA in this complex, if the body of the mRNA is largely naked of proteins, or if there are multiple copies of these components per mRNA, thereby coating the entire length of the transcript. One possibility is that Sbp1p, an abundant RNA binding protein found in yeast P-bodies (Segal et al., 2006), might bind to regions not covered by the Dcp1p–Dcp2p–Edc3p–Dhh1p and Pat1p–Lsm1-7p–Xrn1p complexes. An important issue for future work will be to determine the stoichiometry and spatial arrangement of these complexes with regard to the mRNA, the precise timing of specific interactions, and how the

mRNA is bound by this complex. Moreover, how an mRNA transitions from translation and how that relates to the formation of these complexes with the mRNA remains to be determined. As discussed in the next section, the association of either of the proposed core subcomplexes with an mRNP would provide a potential mechanism for the mRNP to be incorporated into larger scale P-body aggregates via either Edc3p or Lsm4p.

P-body aggregation is mediated by a self-interaction domain of Edc3p and the Q/N-rich C-terminal tail of Lsm4p

Several observations argue that Edc3p functions to aggregate either individual mRNPs or small mRNP complexes into larger microscopically visible P-bodies. First, strains lacking Edc3p show a loss of the small P-bodies seen in mid-log cultures of yeast (Figs. 1 A and 2). Second, the number and size of P-bodies seen in either *dcp1Δ* or *xrn1Δ* strains are reduced in *dcp1Δ edc3Δ* or *xrn1Δ edc3Δ* double mutants (Fig. 1 B). Third, *edc3Δ* cells show defects in P-body aggregation during glucose deprivation and other stresses (Figs. 1 A and 2 and not depicted). Fourth, there is a loss of P-bodies in *lsm4ΔC edc3Δ* strains during glucose deprivation (Fig. 5). Finally, we argue that Edc3p plays a role in the actual assembly of nontranslating mRNPs into larger visible structures because translation repression and mRNA decay are normal in *edc3Δ* strains (Figs. 2 and 6).

The Edc3 protein is a scaffolding protein that provides sites for protein interactions and interconnecting mRNPs. Our results indicate that both the YjeF-N and Lsm domain of Edc3p are required for it being able to contribute to P-body aggregation (Fig. 4). Because the YjeF-N domain interacts with itself (Fig. 3; Fromont-Racine et al., 2000; Marino-Ramirez and Hu, 2002), its function in P-body aggregation is most probably to provide direct interaction between different Edc3p molecules. The role of the Lsm domain is presumably to bind to the Dcp1p–Dcp2p–Dhh1p complex, which would be consistent with the role of Dcp2p in P-body assembly (Teixeira and Parker, 2007). Alternatively, although unlikely given its high degree of divergence, the Lsm domain could oligomerize and/or bind RNA (He and Parker, 2000). The self-interaction of the Yjef-N domain and the interaction of the Lsm domain with mRNA or P-body components provide a cross-bridging mechanism for aggregating mRNPs together. Because Edc3p, its domain organization, and its localization to P-bodies are conserved in eukaryotic cells (Albrecht and Lengauer, 2004; Anantharaman and Aravind, 2004; Kshirsagar and Parker, 2004; Fenger-Gron et al., 2005), one might anticipate that Edc3p will play a role in P-body aggregation in other eukaryotes.

We identified the C-terminal prionlike domain of Lsm4p as another mechanism for the aggregation of mRNPs into microscopically visible P-bodies. The key observation is that *lsm4Δ*C *edc3Δ* strains show a dramatic reduction in P-bodies during glucose deprivation compared with *edc3Δ* strains alone (Fig. 5). In addition, the C-terminal Q/N-rich domain of Lsm4p could be functionally replaced with the Q/N-rich prionlike domain of Rnq1p, a known yeast prion protein (Fig. 5). The simplest model is that when the Lsm1-7p complex is delivered to the mRNA in conjunction with Pat1p (Teixeira and Parker, 2007), the Q/N-rich domain interacts either with itself or other Q/N-rich domains to aggregate mRNPs together in a manner similar to oligomerization of other prion domains, although in this case the aggregation would be readily reversible and not necessarily heritable.

Implications of a prionlike mechanism contributing to P-body aggregation

The contribution of a prionlike domain to yeast P-body assembly is intriguing because of the other 107 proteins in yeast with prionlike domains (Michelitsch and Weissman, 2000); 47 of them are involved in mRNA transport, translation, or degradation or have other connections to RNA metabolism (Table S1 A, available at http://www.jcb.org/cgi/content/full/jcb.200704147/DC1). For example, the yeast P-body components Ccr4p, Pop2p, Not1p, Not4p, Dhh1p, Edc3p, and all five Puf proteins, which regulate mRNA deadenylation and decapping (Wickens et al., 2002), all contain Q/N-rich regions. This abundance of Q/N domains in proteins involved in mRNA metabolism suggests that interactions between these prionlike domains might also contribute in some cases to P-body assembly or other subcellular assemblies of mRNPs.

The role of a prionlike domain in P-body assembly in yeast has three implications for metazoan cells. First, although the prionlike domain of yeast Lsm4p is not conserved, several proteins found in metazoan P-bodies contain conserved Q/N-rich domains, including Dcp2p, Ge-1/Hedls, and GW182 (Table S1 B), although these domains do not always meet the formal criteria for "prion domains" established earlier (Michelitsch and Weissman, 2000). This suggests that aggregation based on Q/N-rich regions will contribute to assembly of P-bodies in metazoans. Second, because Q/N-rich prionlike domains contribute to stress granule formation in mammalian cells (Gilks et al., 2004) and stress granules can merge or dock with P-bodies in human cells (Kedersha et al., 2005; Wilczynska et al., 2005), a reasonable hypothesis is that the juxtaposition of stress granules and P-bodies is mediated by a shared assembly mechanism based on prionlike domains. Finally, because Q/N-rich domains in Pum2 and cytoplasmic polyadenylation element binding protein have been suggested to play roles in the regulation of translation in neurons (Si et al., 2003; Vessey et al., 2006) and at least some neuronal RNA granules are similar to P-bodies (Barbee et al., 2006), one might anticipate that aggregation mechanisms into P-bodies based on Q/N domains will be important in the regulation of translation in neurons.

Efficient P-body aggregation is not required for basic control of mRNA decay and translation repression

Our results argue that formation of microscopically visible P-bodies is not required for the basal control of translation and mRNA degradation. The key observation is that *lsm4ΔC edc3Δ* strains are severely defective in P-body aggregation (Fig. 5) but competent for translation repression during glucose deprivation and show normal mRNA turnover rates (Figs. 5 and 6). The simplest interpretation is that the association of P-body components with an individual mRNA is sufficient for a basal level of translation repression and/or decapping. However, we cannot rule

out the possibility that, in the absence of Edc3p and the prion-like domain of Lsm4p, aggregates too small to detect by the light microscope but nonetheless functional can still form. Consistent with the interpretation that large-scale aggregates do not strongly influence translation repression or mRNA turnover, microscopically visible P-bodies can be depleted in metazoan cells by knockdown of Lsm1p or Lsm3p without affecting miRNA-mediated repression (Chu and Rana, 2006; Eulalio et al., 2007b), knockdown of GW182 without affecting mRNA decay stimulated by AU-rich elements (Stoecklin et al., 2006), or knockdown of any one of several P-body components without affecting nonsense mediated decay (Eulalio et al., 2007b).

An unresolved issue is the function of aggregation of individual mRNPs into larger P-body structures. The conservation of P-bodies strongly argues that the aggregation of nontranslating mRNPs together into larger structures does confer some adaptive function. For example, sequestration might increase the effectiveness of translation repression by limiting the access of the translation machinery to mRNA and reducing the likelihood of disassembly of repression complexes on mRNAs. Thus, aggregation could have a subtle effect on the persistence, or degree of, translation repression and/or decay rates either in general or on a specific subset of mRNA. Alternatively, aggregation could be important for efficient transport of mRNA to specific subcellular regions. Finally, aggregation may be more critical for limiting interactions of nontranslating mRNA with other cellular components. For example, aggregation of such mRNA into P-bodies would presumably limit base pairing between untranslating mRNA and mRNA in polysomes that might be detrimental for translation. Similarly, aggregation into P-bodies may protect untranslating mRNA from degradation by the exosome or influence the specificity of protein interactions with target mRNA by concentrating RNA binding proteins with their targets and limiting their access to off-target mRNA. An important goal of future work will be a thorough analysis of strains specifically deficient in P-body aggregation to determine how mRNA metabolism is now altered.

Materials and methods

Yeast strains, growth conditions, plasmids, and oligonucleotides

Strains used in this study are listed in Table S2 (available at http://www.jcb.org/cgi/content/full/jcb.200704147/DC1). Strains with C-terminal GFP fusion proteins were derived from strains described previously (Sheth and Parker, 2003; Teixeira and Parker, 2007). C-terminal deletion of LSM4 was constructed using a PCR-based protocol (Longtine et al., 1998). The *lsm4Δ edc3Δ* Dcp2GFP strain was constructed from a single cross between yRP2164 and a haploid *lsm4Δ* strain derived from a heterozygous diploid *lsm4Δ* strain (Open Biosystems). Strains were grown at 30°C unless otherwise stated in either yeast extract/peptone medium (YP) or synthetic medium (SC) supplemented with appropriate amino acids and 2% glucose. Respiratory-deficient (petite) derivatives of wild-type or *edc3Δ* strains were obtained by screening for colonies that had spontaneously lost the ability to grow on glycerol. Plasmids and oligonucleotides used in this study are listed in Table S3.

Microscopy

Cultures were grown to OD 600 of 0.3–0.4, collected by centrifugation, washed, and resuspended in SC plus amino acids supplemented with glucose. For glucose depletion in Fig. 1, after washing and resuspension in YP without glucose, cells were incubated in a flask in a shaking water bath for 10 min and washed with SC without glucose. For glucose depletion without aeration, cells were washed and resuspended in SC without glucose and incubated in a microcentrifuge tube. For glucose depletion with aeration, after washing and resuspension in SC without glucose, cells were incubated in a flask in a shaking water bath for 10 min. Images for Fig. 1 were acquired with a confocal microscope (PCM 2000; Nikon) using an objective (Plan Apo 100× 1.4 NA; Nikon) with 3× magnification using a photomultiplier tube (R928; Hamamatsu Photonics) and software (Compix Media). All images are a maximum intensity projection of a z series compilation of 6–10 images performed by Compix software. Images for Figs. 2, 4, and 5 were acquired with a deconvolution microscope (Deltavision RT; Applied Precision) using an objective (UPlan Sapo 100× 1.4 NA; Olympus). They were collected using software (softWoRx) as 512 × 512-pixel files with a camera (CoolSNAP HQ; Photometrics) using 1 × 1 binning. Images are maximum intensity projections of a z series compilation of 15 images made using Image J and have been adjusted to the same contrast range except in Fig. 5 B.

Polysome analysis

Cultures at OD 600 of 0.4–0.6 were split, washed, and resuspended with YP with or without glucose, and then incubated in a shaking water bath at 30°C for 10 min. Cells were harvested by centrifugation at 4,000 rpm for 1 min at 4°C over ice, washed in lysis buffer (10 mM Tris-HCl, pH 7.4, 100 mM NaCl, and 30 mM MgCl2), and stored at −80°C. Lysates were prepared by vortexing cells with glass beads at 4°C in lysis buffer containing 0.5 mg/ml heparin and 1mM DTT and clarified by centrifugation for 2 min at 4,000 rpm at 4°C. 10 A254 units of clarified lysate were loaded on 15–50% sucrose gradients containing 50 mM Tris-HCl, pH 7.0, 50 mM NH_4CL, 12 mM $MgCl_2$, and 1 mM DTT, sedimented in a rotor (SW41; Beckman Coulter) using an ultracentrifuge (L8-M; Beckman Coulter) at 4°C for 2.5 h at 39,000 rpm, and collected while the A254 value was monitored using a continuous flow cell UV detector (UA-6; Teledyne Isco).

Yeast two-hybrid assay

Two-hybrid fusion plasmids were constructed by homologous recombination of PCR products into pOAD or pOBD-2 in yeast strains PJ694a and PJ694α (James et al., 1996) as described previously (Cagney et al., 2000). Two-hybrid plasmids and strains were obtained from the Yeast Resource Center (provided by S. Fields, University of Washington, Seattle, WA). Interactions were measured by β-galactosidase plate assays in diploids containing pOAD and pOBD-2 derivatives.

Protein purification, in vitro protein–protein interaction assays, and Western analysis

Purification of His-Dcp2(1–300)-Flag and His-Dcp2(102–300)-Flag was performed as described previously (She et al., 2006). GST-tagged versions of Dhh1p were expressed in *E. coli* BL-21 and purified as described previously (Cheng et al., 2005), except that only the first purification step on glutathione-Sepharose was performed. The GST-Dhh (46–461) plasmid was provided by H. Song (Institute of Molecular and Cell Biology, Proteos, Singapore). The His-tagged FDF domain of Edc3p was purified from *E. coli* BL-21 (DE3) using His-bind resin (Novagen) after incubation with 1 mg/ml lysozyme for 30 min on ice in 20 mM Tris-HCl, pH 7.9, 500 mM NaCl, and 5 mM imidazole containing complete protease inhibitors without EDTA (Pierce Chemical Co.) followed by sonication. Lysates containing a His-tagged Lsm domain of Edc3p were prepared from *E. coli* BL-21 (DE3) by lysing cells in 20 mM Tris-HCl, pH 7.9, 100 mM NaCl, and 10% glycerol containing 1 mg/ml lysozyme for 30 min followed by sonication and clarification.

Binding reactions were performed at 4°C in binding buffer (50 mM Hepes, pH 7.0, 100 mM NaCl, 1 mM DTT, 2 mM $MnCl_2$, 2 mM $MgCl_2$, 1% Triton X-100 (Fisher Scientific), 10% glycerol, and 10 mg/ml BSA) containing ∼20 ng/μl His-Lsm or His-FDF and 25–67.5 ng/μl GST-Dhh1 or His-Dcp2-Flag proteins. Because of the low concentration of His-Lsm in the extracts, the NaCl concentration was increased to 225 mM. Glutathione-Sepharose 4B (GE Healthcare) and anti-Flag M2 agarose (Sigma-Aldrich) was used to pull down GST-Dhh1 and His-Dcp2-Flag, respectively. Western analysis was performed using polyclonal anti-His antibody (Santa Cruz Biotechnology, Inc.).

Western analysis of Edc3 and Dcp2GFP proteins was performed by preparing extracts from wild-type and *edcΔ* strains expressing Flag-tagged versions of Edc3p. Flag-tagged full-length ΔLsm and ΔFDF Edc3 proteins were detected using anti-Flag M2 monoclonal antibody (Sigma-Aldrich). The ΔYjef-N Edc3 protein was detected using a polyclonal antibody raised in rabbits to a purified His-tagged FDF domain (Cocalico Biologicals) because it co-migrated with a nonspecific band detected by the anti-Flag antibody. Dcp2GFP was detected using anti-GFP antibody (Covance).

mRNA half-life analysis

Cells were grown to OD 600 of 0.3–0.4 in media containing 2% galactose at 30 or 24°C for experiments using *dcp2-7*, and then transcription was repressed by resuspending in media with 4% glucose. Total RNA was extracted (Caponigro et al., 1993), and the amount of MFA2pG mRNA was quantified by Northern analysis with oRP140 (Caponigro and Parker, 1995) using a phosphorimager (Molecular Dynamics). Loading corrections were performed as described previously (Caponigro et al., 1993).

Online supplemental material

Table S1 lists Q/N-rich regions in proteins involved in RNA metabolism and location of conserved Q/N-rich regions in metazoan P-body proteins. Table S2 lists yeast strains used in this paper. Table S3 lists plasmids and oligonucleotides used in this paper. Fig. S1 shows the effect of Edc3p domain deletions on Dhh1GFP foci. Fig. S2 shows levels of mutant Edc3p proteins and Dcp2GFP. Online supplemental material is available at http://www.jcb.org/cgi/content/full/jcb.200704147/DC1.

We thank the Parker laboratory and Anne Webb for assistance and discussion and Haiwei Song for reagents. Reagents for two-hybrid assays were provided by S. Fields through the Yeast Resource Center, which is supported by grant P41 RR1183 from the National Center for Research Resources at the National Institutes of Health.

National Institutes of Health grant R37 GM45443 and funds from the Howard Hughes Medical Institute supported this work. D. Teixeira was supported by Fundacao para a Ciencia e Tecnologia (grant SFRH/BD/2739/2000).

Submitted: 25 April 2007
Accepted: 3 October 2007

References

Albrecht, M., and T. Lengauer. 2004. Novel Sm-like proteins with long C-terminal tails and associated methyltransferases. *FEBS Lett.* 569:18–26.

Anantharaman, V., and L. Aravind. 2004. Novel conserved domains in proteins with predicted roles in eukaryotic cell-cycle regulation, decapping and RNA stability. *BMC Genomics*. 5:45.

Anderson, P., and N. Kedersha. 2006. RNA granules. *J. Cell Biol.* 172:803–808.

Andrei, M.A., D. Ingelfinger, R. Heintzmann, T. Achsel, R. Rivera-Pomar, and R. Luhrmann. 2005. A role for eIF4E and eIF4E-transporter in targeting mRNPs to mammalian processing bodies. *RNA*. 11:717–727.

Barbee, S.A., P.S. Estes, A.M. Cziko, J. Hillebrand, R.A. Luedeman, J.M. Coller, N. Johnson, I.C. Howlett, C. Geng, R. Ueda, et al. 2006. Staufen- and FMRP-containing neuronal RNPs are structurally and functionally related to somatic P bodies. *Neuron*. 52:997–1009.

Bhattacharyya, S.N., R. Habermacher, U. Martine, E.I. Closs, and W. Filipowicz. 2006. Relief of microRNA-mediated translational repression in human cells subjected to stress. *Cell*. 125:1111–1124.

Bouveret, E., G. Rigaut, A. Shevchenko, M. Wilm, and B. Seraphin. 2000. A Sm-like protein complex that participates in mRNA degradation. *EMBO J.* 19:1661–1671.

Brengues, M., D. Teixeira, and R. Parker. 2005. Movement of eukaryotic mRNAs between polysomes and cytoplasmic processing bodies. *Science*. 310:486–489.

Cagney, G., P. Uetz, and S. Fields. 2000. High-throughput screening for protein-protein interactions using two-hybrid assay. *Methods Enzymol.* 328:3–14.

Caponigro, G., and R. Parker. 1995. Multiple functions for the poly(A)-binding protein in mRNA decapping and deadenylation in yeast. *Genes Dev.* 9:2421–2432.

Caponigro, G., D. Muhlrad, and R. Parker. 1993. A small segment of the MAT alpha 1 transcript promotes mRNA decay in *Saccharomyces cerevisiae*: a stimulatory role for rare codons. *Mol. Cell. Biol.* 13:5141–5148.

Cheng, Z., J. Coller, R. Parker, and H. Song. 2005. Crystal structure and functional analysis of DEAD-box protein Dhh1p. *RNA*. 11:1258–1270.

Chu, C.Y., and T.M. Rana. 2006. Translation repression in human cells by microRNA-induced gene silencing requires RCK/p54. *PLoS Biol.* 4:e210.

Coller, J., and R. Parker. 2005. General translational repression by activators of mRNA decapping. *Cell*. 122:875–886.

Cougot, N., S. Babajko, and B. Seraphin. 2004. Cytoplasmic foci are sites of mRNA decay in human cells. *J. Cell Biol.* 165:31–40.

Decker, C.J., and R. Parker. 1993. A turnover pathway for both stable and unstable mRNAs in yeast: evidence for a requirement for deadenylation. *Genes Dev.* 7:1632–1643.

Derkatch, I.L., M.E. Bradley, J.Y. Hong, and S.W. Liebman. 2001. Prions affect the appearance of other prions: the story of [PIN(+)]. *Cell*. 106:171–182.

Eulalio, A., I. Behm-Ansmant, and E. Izaurralde. 2007a. P bodies: at the crossroads of post-transcriptional pathways. *Nat. Rev. Mol. Cell Biol.* 8:9–22.

Eulalio, A., I. Behm-Ansmant, D. Schweizer, and E. Izaurralde. 2007b. P-body formation is a consequence, not the cause of RNA-mediated gene silencing. *Mol. Cell. Biol.* 27:3970–3981.

Fenger-Gron, M., C. Fillman, B. Norrild, and J. Lykke-Andersen. 2005. Multiple processing body factors and the ARE binding protein TTP activate mRNA decapping. *Mol. Cell*. 20:905–915.

Ferraiuolo, M.A., S. Basak, J. Dostie, E.L. Murray, D.R. Schoenberg, and N. Sonenberg. 2005. A role for the eIF4E-binding protein 4E-T in P-body formation and mRNA decay. *J. Cell Biol.* 170:913–924.

Fox, T.D., L.S. Folley, J.J. Mulero, T.W. McMullin, P.E. Thorsness, L.O. Hedin, and M.C. Costanzo. 1991. Analysis and manipulation of yeast mitochondrial genes. *Methods Enzymol.* 194:149–165.

Fromont-Racine, M., A.E. Mayes, A. Brunet-Simon, J.C. Rain, A. Colley, I. Dix, L. Decourty, N. Joly, F. Ricard, J.D. Beggs, and P. Legrain. 2000. Genome-wide protein interaction screens reveal functional networks involving Sm-like proteins. *Yeast*. 17:95–110.

Gavin, A.C., P. Aloy, P. Grandi, R. Krause, M. Boesche, M. Marzioch, C. Rau, L.J. Jensen, S. Bastuck, B. Dumpelfeld, et al. 2006. Proteome survey reveals modularity of the yeast cell machinery. *Nature*. 440:631–636.

Gilks, N., N. Kedersha, M. Ayodele, L. Shen, G. Stoecklin, L.M. Dember, and P. Anderson. 2004. Stress granule assembly is mediated by prion-like aggregation of TIA-1. *Mol. Biol. Cell*. 15:5383–5398.

He, W., and R. Parker. 2000. Functions of Lsm proteins in mRNA degradation and splicing. *Curr. Opin. Cell Biol.* 12:346–350.

Holmes, L.E., S.G. Campbell, S.K. De Long, A.B. Sachs, and M.P. Ashe. 2004. Loss of translational control in yeast compromised for the major mRNA decay pathway. *Mol. Cell. Biol.* 24:2998–3010.

Jakymiw, A., S. Lian, T. Eystathioy, S. Li, M. Satoh, J.C. Hamel, M.J. Fritzler, and E.K. Chan. 2005. Disruption of GW bodies impairs mammalian RNA interference. *Nat. Cell Biol.* 7:1267–1274.

James, P., J. Halladay, and E.A. Craig. 1996. Genomic libraries and a host strain designed for highly efficient two-hybrid selection in yeast. *Genetics*. 144:1425–1436.

Kedersha, N., G. Stoecklin, M. Ayodele, P. Yacono, J. Lykke-Andersen, M.J. Fritzler, D. Scheuner, R.J. Kaufman, D.E. Golan, and P. Anderson. 2005. Stress granules and processing bodies are dynamically linked sites of mRNP remodeling. *J. Cell Biol.* 169:871–884.

Kshirsagar, M., and R. Parker. 2004. Identification of Edc3p as an enhancer of mRNA decapping in *Saccharomyces cerevisiae*. *Genetics*. 166:729–739.

Liu, J., M.A. Valencia-Sanchez, G.J. Hannon, and R. Parker. 2005. MicroRNA-dependent localization of targeted mRNAs to mammalian P-bodies. *Nat. Cell Biol.* 7:719–723.

Longtine, M.S., A. McKenzie, D.J. Demarini, N.G. Shah, A. Wach, A. Brachat, P. Philippsen, and J.R. Pringle. 1998. Additional modules for versatile and economical PCR-based gene deletion and modification in *Saccharomyces cerevisiae*. *Yeast*. 14:953–961.

Marino-Ramirez, L., and J.C. Hu. 2002. Isolation and mapping of self-assembling protein domains encoded by the *Saccharomyces cerevisiae* genome using lambda repressor fusions. *Yeast*. 19:641–650.

Michelitsch, M.D., and J.S. Weissman. 2000. A census of glutamine/asparagine-rich regions: implications for their conserved function and the prediction of novel prions. *Proc. Natl. Acad. Sci. USA*. 97:11910–11915.

Parker, R., and U. Sheth. 2007. P bodies and the control of mRNA translation and degradation. *Mol. Cell*. 25:635–646.

Pauley, K.M., T. Eystathioy, A. Jakymiw, J.C. Hamel, M.J. Fritzler, and E.K. Chan. 2006. Formation of GW bodies is a consequence of microRNA genesis. *EMBO Rep.* 7:904–910.

Pillai, R.S., S.N. Bhattacharyya, C.G. Artus, T. Zoller, N. Cougot, E. Basyuk, E. Bertrand, and W. Filipowicz. 2005. Inhibition of translational initiation by Let-7 MicroRNA in human cells. *Science*. 309:1573–1576.

Segal, S.P., T. Dunckley, and R. Parker. 2006. Sbp1p affects translation repression and decapping in *Sacharomyces cerevisiae*. *Mol. Cell. Biol.* 26:5120–5130.

Seydoux, G., and R.E. Braun. 2006. Pathway to totipotency: lessons from germ cells. *Cell*. 127:891–904.

She, M., C.J. Decker, N. Chen, S. Tumati, R. Parker, and H. Song. 2006. Crystal structure and functional analysis of Dcp2p from *Schizosaccharomyces pombe*. *Nat. Struct. Mol. Biol.* 13:63–70.

Sheth, U., and R. Parker. 2003. Decapping and decay of messenger RNA occur in cytoplasmic processing bodies. *Science*. 300:805–808.

Sheth, U., and R. Parker. 2006. Targeting of aberrant mRNAs to cytoplasmic processing bodies. *Cell*. 125:1095–1109.

Si, K., S. Lindquist, and E.R. Kandel. 2003. A neuronal isoform of the aplysia CPEB has prion-like properties. *Cell*. 115:879–891.

Sondheimer, N., and S. Lindquist. 2000. Rnq1: an epigenetic modifier of protein function in yeast. *Mol. Cell*. 5:163–172.

Steiger, M., A. Carr-Schmid, D.C. Schwartz, M. Kiledjian, and R. Parker. 2003. Analysis of recombinant yeast decapping enzyme. *RNA*. 9:231–238.

Stoecklin, G., T. Mayo, and P. Anderson. 2006. ARE-mRNA degradation requires the 5′-3′ decay pathway. *EMBO Rep.* 7:72–77.

Teixeira, D., and R. Parker. 2007. Analysis of P-body assembly in *Saccharomyces cerevisiae*. *Mol. Biol. Cell*. 18:2274–2287.

Teixeira, D., U. Sheth, M.A. Valencia-Sanchez, M. Brengues, and R. Parker. 2005. Processing bodies require RNA for assembly and contain nontranslating mRNAs. *RNA*. 11:371–382.

Tharun, S., W. He, A.E. Mayes, P. Lennertz, J.D. Beggs, and R. Parker. 2000. Yeast Sm-like proteins function in mRNA decapping and decay. *Nature*. 404:515–518.

Unterholzner, L., and E. Izaurralde. 2004. SMG7 acts as a molecular link between mRNA surveillance and mRNA decay. *Mol. Cell*. 16:587–596.

Vessey, J.P., A. Vaccani, Y. Xie, R. Dahm, D. Karra, M.A. Kiebler, and P. Macchi. 2006. Dendritic localization of the translational repressor Pumilio 2 and its contribution to dendritic stress granules. *J. Neurosci.* 26:6496–6508.

Wickens, M., D.S. Bernstein, J. Kimble, and R. Parker. 2002. A PUF family portrait: 3′UTR regulation as a way of life. *Trends Genet.* 18:150–157.

Wilczynska, A., C. Aigueperse, M. Kress, F. Dautry, and D. Weil. 2005. The translational regulator CPEB1 provides a link between dcp1 bodies and stress granules. *J. Cell Sci.* 118:981–992.